# Control Design of Anti-Roll Bar Actuator Based on Constrained LQ Method

Balázs Varga, Balázs Németh and Péter Gáspár

*Abstract*—The paper proposes the modeling and control design of an active anti-roll bar actuator. The vehicle dynamic system improves the roll stability of a light commercial vehicle generating an active torque on the chassis, provided by an electro-hydraulic actuator. The actuator control system must guarantee the generation of the required active torque, satisfying the input limits of the actuator. The actuation of electro-hydraulic system is described by fluid dynamical, electrical and mechanical equations. The input of the formulated state-space actuator model is the valve current, while the output is the generated active torque. The tracking controller of the actuator is designed based on constrained Linear Quadratic (LQ) method. The designed controller guarantees the tracking performance and the avoidance of constraint violation simultaneously. The operation of the designed control system is illustrated through simulation examples.

## I. Introduction and Motivation

Improvement of roll dynamics is a relevant problem at vehicles with high center of gravity. Several roll control systems are developed, which enhances the protection of cargo and improves roll stability. One of the most preferred roll control solution is anti-roll bar, which is often used in light commercial vehicles, buses, trucks. In this control system two torsion bars connect the left and the right suspensions on an axle.

Active anti-roll bars have numerous advantages over the passive anti-roll systems used nowadays. Although passive anti-roll systems can enhance the roll dynamics of the vehicle, is results a performance degradation on traveling comfort. The active system is also able to adapt to the actual road conditions and lateral effects, while the roll stability is improved.

The active system proposed in this paper integrates an electro-hydraulic actuator into an anti-roll bar. The system consists of an upper-level controller which improves the roll dynamics of the chassis. The actuator of the anti-roll bar is an oscillating hydromotor with a servo valve on the lower-level. The goal of the paper is the control design of the electro-hydraulic actuator. The actuator control guarantees the generation of the necessary active torque and satisfies the input constraint of the electric circuit. The control design is based on a constrained LQ method [1].

Several papers propose methods to reduce the chassis roll motion of heavy vehicles. Three different active systems are applied, such as anti-roll bar, additional steering and differential braking [2], [3]. Active anti-roll bars commonly employ hydraulic actuators to achieve this goal, see [4], [5], [6]. In [7] an active roll control system based on a modified suspension system is developed with distributed control architecture. Active steering uses an auxiliary steering angle to reduce the rollover risk of the vehicle. However, this method also influences the lateral motion of the vehicle significantly, see [8], [9]. An advantage of differential braking technique is the simple construction and low cost, see [10]. In this case different braking forces are generated on the wheels to reduce the lateral force. Therefore the rollover of the vehicle can be avoided. Several papers deal with the integration of the previous systems. In [2] the integration of active anti-roll bar and active braking is presented. [11] proposes a reconfigurable control algorithm to prevent rollover of heavy vehicles. [12] investigates the coordination of active control systems could be controlled to alter the vehicle rollover tendencies.

The paper is organized as follows. Section II presents the formulation of chassis roll dynamics. The control-oriented modeling of the electro-hydraulic actuator using fluid dynamical, electrical and mechanical equations is proposed in Section III. Section IV describes the architecture of the active anti-roll bar control system. Section V introduces the constrained LQ controller design of the actuator and illustrates the system operation. Actuation of the control system is illustrated by a simulation example in Section VI. Finally, Section VII concludes the contributions of the paper.

## II. Modeling of chassis roll dynamics

In this section the roll dynamics of the chassis is described, which is enhanced by the active anti-roll bar system. The four degree-of-freedom dynamical model of a light commercial vehicle is illustrated in Figure 1. Since this type of vehicle has a high center of gravity, the rolling motion of the chassis (sprung mass) is significant. Thus, the protection of the cargo requires an anti-roll bar system, which reduces the chassis roll angle.

The intervention of the anti-roll bar system is a force couple on the unsprung masses, which is provided by an active torque of the electro-hydraulic actuator $M_{act}$. Lateral force $F_{lat}$ on the vehicle chassis and road excitations on the wheels $g_{01}$, $g_{02}$ are disturbances of the system. In the linear model the masses, spring stiffness, damping ratios and geometrical parameters are constants. $h$ is the distance between the roll center of chassis and its center of gravity and $r$ is half-track of the vehicle, see Figure 1. The length of the anti-roll bar arm in longitudinal direction is noted with $a$. In the model the effects of side-slip angle and under-/oversteering are neglected.

Varga, Németh and Gáspár are with Systems and Control Laboratory, Institute for Computer Science and Control, Hungarian Academy of Sciences, Kende u. 13-17, H-1111 Budapest, Hungary. E-mail: [bvarga;bnemeth;gaspar]@sztaki.mta.hu
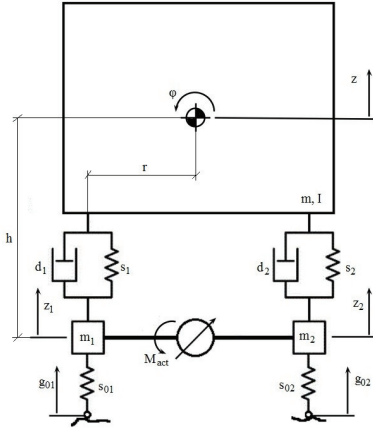
Fig. 1. Proposed vehicle model

The dynamics of roll motion are derived from the Euler-Lagrange equations. Four second-order differential equations are formulated as shown below (1). (1a) describes the vertical dynamics of the sprung mass $m$, while its roll dynamics is described in (1b). The vertical dynamics of the unsprung masses $m_1$, $m_2$ are expressed in (1c) and (1d).

$$
m\ddot{z} = - (d_1 + d_2)\dot{z} - (d_2 r - d_1 r)\dot{\varphi} + d_1\dot{z}_1 + d_2\dot{z}_2
$$
$$
- (s_1 + s_2)z - (s_2 r - s_1 r)\varphi + s_1 z_1 + s_2 z_2 \quad (1a)
$$
$$
I\ddot{\varphi} = - (d_2 - d_1)r\dot{z} - (d_1 + d_2)r^2\dot{\varphi} - d_1 r\dot{z}_1
$$
$$
+ d_2 r\dot{z}_2 - (s_2 - s_1)rz - (s_1 + s_2)r^2\varphi
$$
$$
- s_1 r z_1 + s_2 r z_2 + F_{lat}h \quad (1b)
$$
$$
m_1\ddot{z}_1 = d_1\dot{z} - d_1 r\dot{\varphi} - d_1\dot{z}_1 + s_1 z + s_1 r\varphi
$$
$$
- (s_1 + s_{01})z_1 + s_{01}g_{01} + \frac{M_{act}}{2a} \quad (1c)
$$
$$
m_2\ddot{z}_2 = d_2\dot{z} + d_2 r\dot{\varphi} - d_2\dot{z}_2 + s_2 z - s_2 r\varphi
$$
$$
- (s_2 + s_{02})z_2 + s_{02}g_{02} - \frac{M_{act}}{2a} \quad (1d)
$$

The proposed dynamical equations (1) are transformed into state-space form as:

$$
\dot{x} = Ax + B_1 w + B_2 u \quad (2)
$$

where the state vector of the system $x = \begin{bmatrix} z_1 & z_2 & z & \phi & \dot{z}_1 & \dot{z}_2 & \dot{z} & \dot{\phi} \end{bmatrix}^T$ incorporates the vertical displacements of unsprung masses $z_1$, $z_2$ and sprung masses $z$, the chassis roll angle $\phi$ and their derivatives. The control input $u = M_{act}$ of the system is the active torque generated by the electro-hydraulic actuator. The disturbances $w = \begin{bmatrix} g_{01} & g_{02} & F_{lat} \end{bmatrix}^T$ of the system are road excitations on the wheel and lateral forces. The formulated state-space model of the chassis roll dynamics is the basis of the upper-level control design, see Section IV.

## III. ELECTRO-HYDRAULIC ACTUATOR MODEL OF ANTI-ROLL BAR SYSTEM

In the previous section the roll motion of the chassis is formulated and the dynamical effect of the anti-roll bar is

presented. The active torque $M_{act}$ is generated by the electro-hydraulic actuator, proposed in the followings.

The actuator that realizes the torque required to enhance the roll stability of the vehicle is an oscillating hydromotor, see Figure 2. An oscillating hydromotor is a rotary actuator with two cells, separated by vanes. The pressure difference between the vanes generates a torque on the central shaft, which has a limited rotation angle. The anti-roll bar is split in two halves and the motor couples them. The shaft of the motor is connected to one side of the roll bar and the housing is to the other. When the vehicle chassis rolls, a torque appears in the house which can be countered by the pressure difference in the two chambers provided by a pump. The hydromotor is connected to a symmetric 4/2 four way valve, the spool displacement of this valve is realized by a permanent magnet flapper motor. Since the presented system has a high energy density, it requires small space and it has low mass. Besides, the actuator has a simple construction, but it requires an external high pressure pump [13].
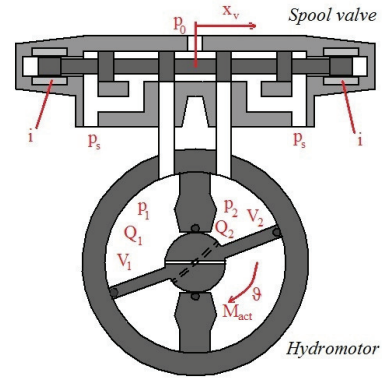


Fig. 2. Electro-hydraulic actuator

The physical input of the actuator is the valve current $i$, the output is the active torque $M_{act}$. The flapper motor and the spool can be modeled as a second order linear system, which creates a linear dependence between the valve current and the spool displacement. In this formulation the nonlinear friction is neglected. The motion of valve is modeled as:

$$
\frac{1}{\omega_v^2}\ddot{x}_v + \frac{2D_v}{\omega_v}\dot{x}_v + x_v = k_v i \quad (3)
$$

where $k_v$ valve gain equals

$$
k_v = \frac{Q_N}{\sqrt{\Delta p_N/2}}\frac{1}{u_{vmax}} \quad (4)
$$

$Q_N$ is the rated flow at rated pressure and maximum input current, $p_N$ is the pressure drop at rated flow and $u_{vmax}$ is the max rated current. $D_v$ is the valve damping coefficient, which can be calculated from the apparent damping ratio. $D_v$ stands for the natural frequency of the valve [14]

The pressures in the chambers depend on the flows of the circuits $Q_1$, $Q_2$. $p_L$ is the load pressure difference between

the two chambers. The average flow of the system, assuming the supply pressure $p_s$ is constant:

$$Q_L(x_v, p_L) = C_d A(x_v)\sqrt{\frac{1}{\rho}(p_s - \frac{x_v}{|x_v|}p_L)} \qquad (5)$$

This equation can be linearized around $(x_{v,0}; p_{L,0})$ such as [13]

$$Q_L = K_q x_v - K_c p_L \qquad (6)$$

where $K_q$ is the valve flow gain coefficient and $K_c$ is the valve pressure coefficient. In this modeling principle, the hydromotor model does not take into account the friction force and the external leakage flow. The compressibility of the fluid is considered constant [13].

The volumetric flow in the chambers is formed as

$$\dot{p}_L = \frac{4\beta_E}{V_t}(Q_L - V_p\vartheta + c_{l1}\dot{\vartheta} - c_{l2}p_L) \qquad (7)$$

where $\beta_E$ is the effective bulk modulus, $V_t$ is the total volume under pressure and $V_p$ is proportional to the areas of vane cross-sections. $c_{l1}$ and $c_{l2}$ are parameters of the leakage flow.

The motion equation of the shaft rotation due to the pressure difference $\dot{p}_L$ and the external load $M_{ext}$:

$$J\ddot{\vartheta} = -d_a\dot{\vartheta} + V_p p_L + M_{ext} \qquad (8)$$

where $J$ is the mass of the hydromotor shaft and vanes, $d_a$ is the damping constant of the system. $M_{ext}$ is the effect of disturbances on the chassis roll dynamics.

The active torque of the actuator is determined by $p_L$. The relationship is written as follows:

$$M_{act} = 2p_L A_v a \qquad (9)$$

where $A_v$ is the area of the vanes and $a$ is the arm of the stabilizer bar in longitudinal direction.

The control design of the actuator requires transformation of the previous equations in state-space form. (3), (7) and (8) are the necessary differential equations, (6) is the part of (7):

$$\dot{x}_{act} = A_{act}x_{act} + B_{act,1}w_{act} + B_{act,2}u_{act} \qquad (10a)$$
$$y_{act} = c_{act}x_{act} \qquad (10b)$$

The state vector of the actuator model $x_{act} = \begin{bmatrix} x_v & \dot{x}_v & p & \vartheta \end{bmatrix}^T$ contains the spool displacement $x_v$ and its derivative $\dot{x}_v$, the load pressure $p$ and the shaft angular velocity $\dot{\vartheta}$. The output $y_{act} = M_{act}$ of the system is formulated using (9). The control input is $u_{act} = i$, while the disturbance is the external load $w_{act} = M_{ext}$.

## IV. Hierarchical Concept of Anti-Roll Bar Control Design

In the previous section the roll dynamics and the electro-hydraulic actuator have been modeled for active anti-roll bar control design. In the followings the architecture of the control system is presented.

The hierarchical architecture of the control systems is illustrated in Figure 3. Two control levels are distinguished in this scheme: an upper- and a lower-level. The two levels are
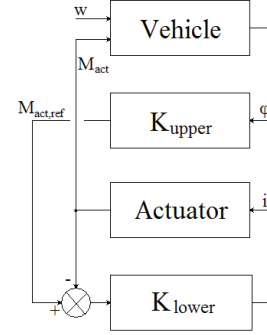


Fig. 3. Architecture of control systems

interconnected during the vehicle dynamics and the reference signal. The aim of the upper-level controller $K_{upper}$ is to guarantee the vehicle dynamic performances, e.g. chassis roll angle minimization. The control input of the upper-level controller is the reference active torque $M_{act,ref}$, which must be realized by actuator. The tracking of $M_{act,ref}$ is guaranteed by the lower-level controller $K_{lower}$, which computes a valve current $i$ for the electro-hydraulic actuator. The advantage of hierarchical design is the independent design of the controllers on the different levels. Thus, the controllers can be designed for subsystems with smaller complexity. However, in case of the independent control design the global stability of the controlled interconnected system has to be ensured by the existence of a Common Lyapunov Function. Further details about hierarchical control design is found in [15].

In the paper the focus is on the design of the lower-lever anti-roll bar controller, proposed in the next section. Several methods and control design have been published about the vehicle dynamic control systems, which can be applied for upper-level anti-roll bar controller design. Since the parameters of the vehicle model are uncertain and the model contains neglected dynamics, robust control design techniques are used for control design in several papers, see e.g. [16]. The theoretical principles of robust control design is found in [17]. [15] proposes the application of robust control techniques for automotive vertical dynamical applications such as roll control. The nonlinear dynamics of the roll motion is handled using the Linear Parameter Varying (LPV) control concept in [18]. In the paper the LPV method of [19] is used for upper-level control design.

## V. Actuator Level Control Design

In this section the torque tracking lower-level actuator control design is proposed based on the constrained Linear Quadratic (LQ) control design method. The aim of the controller is to guarantee the required active torque of the upper-lever vehicle dynamic controller and satisfy the input constraint of the lower-level.

The lower-level LQ controller is based on a piecewise linear control strategy. This method can be used for the approxi-

mation of nonlinear systems using linear sections. Piecewise linear systems are special types of switched linear systems with state-space partition-based switching. The main difficulty of this strategy is the switching between the controllers, which can causes transients in the control system [20].

The aim of the actuator control design is to guarantee the reference active torque signal computed by the upper-level controller. Thus, the lower-level control system must satisfy the following performance:

$$z = M_{act,ref} - M_{act}; \qquad |z| \rightarrow min \qquad (11)$$

The tracking criterion of the control system requires the reformulation of the state-space equation described in (10). The plant is augmented with an integrator on signal $M_{act}$ to achieve zero steady-state error. The augmented system is written as follows:

$$\begin{bmatrix} \dot{x}_{act} \\ \dot{z} \end{bmatrix} = \begin{bmatrix} A_{act} & 0 \\ -c_{act} & 0 \end{bmatrix} \begin{bmatrix} x_{act} \\ z \end{bmatrix} + \\ + \begin{bmatrix} B_{act,1} \\ 0 \end{bmatrix} w_{act} + \begin{bmatrix} B_{act,2} \\ 0 \end{bmatrix} u_{act} + \begin{bmatrix} 0 \\ 1 \end{bmatrix} M_{act,ref} \qquad (12)$$

Another criterion of the system is the minimization of control input, such as:

$$|u_{act}| = |i| \rightarrow min \qquad (13)$$

The reduction of the control input is necessary to have an effect on input constraint satisfaction.

The LQ controller design is based on the minimization of the following cost function, which incorporates the previous conditions (11) and (13):

$$J = \frac{1}{2} \int_0^\infty \left[ \tilde{x}_{act}^T Q \tilde{x}_{act} + Ri^2 \right] dt \rightarrow min \qquad (14)$$

where $\tilde{x}_{act} = \begin{bmatrix} x_{act} & z \end{bmatrix}^T$. The weights $Q$ and $R$ guarantee a balance between the performances. These weights have an important role to satisfy input constraints, as seen below. The minimization problem leads to a continuous time algebraic Riccati equation (CARE) [17]:

$$P\tilde{A}_{act} + \tilde{A}_{act}^T P - P\tilde{B}_{act,2} R^{-1} \tilde{B}_{act,2}^T P + Q = 0 \qquad (15)$$

where $P$ is the solution of CARE, $\tilde{A}_{act}$ and $\tilde{B}_{act,2}$ are the block matrices of (12). The optimal state feedback LQ controller $K_{lower}$ is derived from $P$.

Since the electric circuit of the actuator has physical limits, it is necessary to guarantee the avoidance of the valve current increase over a limit $u_{const}$. In the conventional formulation of LQ problem (14) it can be ensured by a high $R$ weight. It results a conservative $K_{lower}$ controller with small gain, which leads to a reduced control input and the degradation of $z$ tracking performance simultaneously. On the other hand, large LQ gain enhances the tracking performance, but it will likely violate the input constraint $u_{const}$. A way to guarantee the (11) and input constraint satisfaction is presented in [1]. In this paper an iterative LQ control design method is proposed, which results a switching LQ controller. In the

method numerous controllers are designed using different $R$ weights. The iterative function for control design is written as follows:

$$R_i = \frac{\sqrt{\rho_i}}{u_{const}} \sqrt{(B^T P_{i-1} B)} \qquad (16)$$

In the method the different $R_i$ weights are used at fixed $Q$ matrices. $\rho_i$ is the actual gain scaling parameter and $u_{const}$ is the input constraint, must be satisfied. $P_{i-1}$ is the solution of the $(i-1)^{th}$ Ricatti equation (15).

The solution of $i^{th}$ CARE is $P_i$, from which the $i^{th}$ optimal LQ control can be computed. Besides, $P_i$ determines an ellipsoidal invariant set $\varepsilon_i$ in the state-space, where the input constraint can be satisfied. As a result of the iterative design, numerous LQ gains and invariant sets are computed. The controller with the largest LQ gain belongs to the smallest ellipsoid. Based on the invariant sets, a switching strategy is defined to guarantee the input constraint. In the strategy the trajectory of $\tilde{x}_{act}$ is monitored. When the trajectory reaches the set border of an ellipsoid and moves outwards, the system switches to a more conservative controller with smaller LQ gain. The switching function is formulated as follows:

$$sign\left(\rho_i - \tilde{x}_{act}^T P_i \tilde{x}_{act}\right) < 1 \qquad (17)$$

If (17) is not satisfied, then $\tilde{x}_{act}$ is out of the $i^{th}$ ellipsoid, thus it is necessary to switch to the $(i-1)^{th}$ controller. The solution of the switching algorithm is always the smallest ellipsoid, which contains $\tilde{x}_{act}$. In the method it is necessary to guarantee that $\tilde{x}_{act}$ never departs the largest ellipsoid $\varepsilon_1$. Therefore $\rho_1$ must be chosen high enough not to violate this condition. Since the system states are always in the outermost invariant set, the stability of the system is guaranteed. The switching algorithm described above is illustrated in Figure 4.
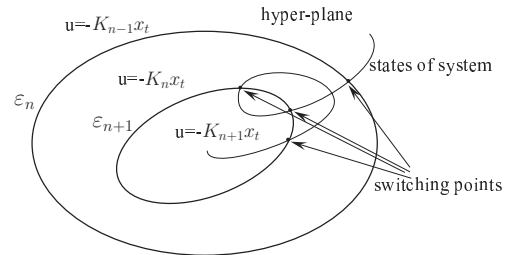


Fig. 4. Invariant sets and switching of the two-state system

*Remark 1:* If the matrices of the system (12) are ill-conditioned, or the dimension of the system is high, at the solution of (15) numerical problems can occur. In this case the control design must to be adapted to the $R_i$ weights, where a solution of CARE exists. The $\rho_i$ parameters must be calculated from $R_i$ using (16) and the sizes of the ellipsoids are tuned manually.

*A. Illustration of constrained LQ control*

In the followings an illustration of the constrained LQ control during a simulation example is shown. Since the

switching between controllers is based on ellipse invariant sets, a two-dimensional system is chosen for the illustration (18). In this scenario the switching events can be illustrated in a 2D plane. The system has two states in a state vector $x = \begin{bmatrix} x_1 & x_2 \end{bmatrix}^T$, control input $u$ and disturbance signal $w$:

$$\dot{x} = \begin{bmatrix} -5 & -1 \\ 1 & 0 \end{bmatrix} x + \begin{bmatrix} 1 \\ 0 \end{bmatrix} u + \begin{bmatrix} 1 \\ 0 \end{bmatrix} w \qquad (18)$$

Six LQ controllers $n = 1 \dots 6$ are designed by the presented method. The input constraint of the system is $|u_{const}| = 1$.

The simulation results of the system (18) is found in Figure 5. Three scenarios are compared: the proposed switching LQ method and two constant LQ controls. $n = 1$ LQ control is related to the smallest gain of the switching control sequence, which satisfies the input constraint. Since the gain of $n = 1$ LQ controller is small, the performance of the system is reduced. It corresponds to a conservative control. $n = 6$ LQ belongs to the highest gain of the switching control sequence. In this case the performance of the system is improved, but the input constraint is violated.

The performance of the system is the minimization of state $x_2$. The initial states of the systems are $x_0 = \begin{bmatrix} 0;0 \end{bmatrix}^T$. The disturbance signal of the system is shown in Figure 5(a). The aim of the control system is to minimize $x_2$ against the disturbance, see Figure 5(b). It can be seen that $n = 6$ LQ controller is able to minimize $x_2$, however $|u_{const}| = 1$ is violated, see Figure 5(c). The controller $n = 1$ LQ satisfies the input constraint, but it leads to the degradation of the performance. An appropriate balance between the two constant gain LQ controllers is the proposed switching LQ. In case of the switching LQ the input constraint is satisfied, see Figure 5(c) between $0s \dots 25s$. When the required control input is decreased, the performance of the system is improved e.g. between $25s \dots 50s$. The balance between the control input limitation and performance improvement is guaranteed by the switching strategy, see Figure 5(d). The influence of invariant sets on the state trajectory of switching LQ controller is illustrated in Figure 5(e). The direction of the trajectory is modified at achievements of the set borders. It is resulted by the switching between LQ controllers.

## VI. SIMULATION EXAMPLE

In this section the operation of the active anti-roll bar is presented during a simulation example. The constrained LQ control design and the system model is performed by Matlab/Simulink. In the simulation a light commercial vehicle is analyzed, of which mass is $3500 kg$ altogether with sprung and unsprung masses. The difference between chassis roll center and center of gravity is $h = 1000mm$. In the example the focus is on the efficiency of the lower-level actuator control. Seven LQ gains are designed in the example: $n = 1$ LQ control has the highest gain, which improves the tracking performance; while $n = 7$ is the most conservative, which satisfies the constraint.

In the example the vehicle travels along a straight road with constant velocity. The road excitation modifies the roll of the

(a) Disturbance

(b) Performance

(c) Control input

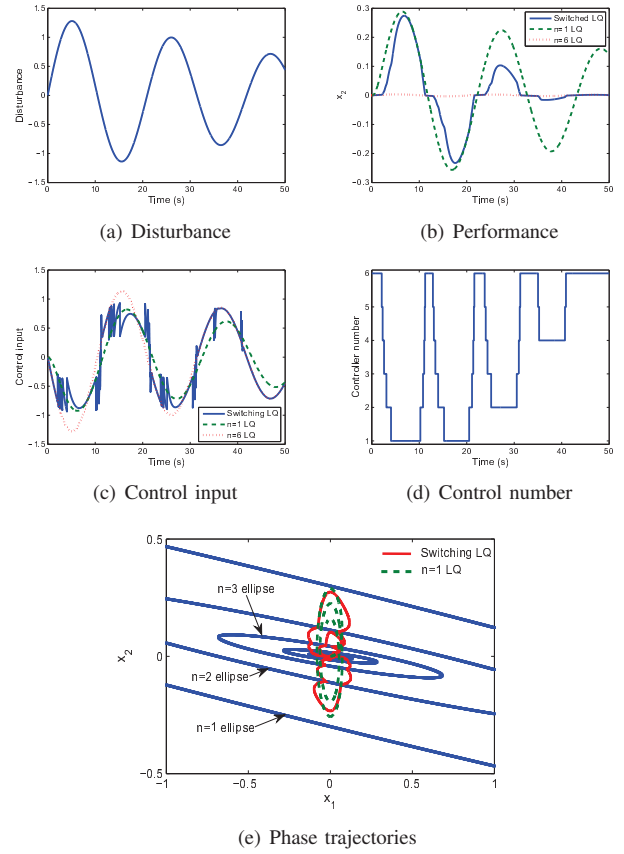(d) Control number

(e) Phase trajectories

Fig. 5. Simulation results of the proposed simple system

chassis during the course. In the scenario the disturbance of the system is a stochastic road excitation with a zero mean value and a $0.05m$ standard deviation, see Figure 6(a). The upper-level controller computed reference active torque $M_{act,ref}$ to minimize the roll angle. $M_{act}$ must be generated by the actuator using the lower-level controller. The tracking performance of the actuator control system is shown in Figure 6(b). In Figure 6(c) can be seen the control input of the actuator $i$. The input constraint of the system is $|u_{const}| = 0.3A$. Since the input constraint must be satisfied, the controller switches to a more conservative LQ gain, when the limit is reached, see Figure 6(d). In the example the input constraint is not violated, thus the limit is not violated. Figure 6(b) shows that the controller guarantees the tracking of the reference torque with an appropriate threshold. However, around $5s$ and $30s$ the tracking error is increased. In these cases the controller gain is modified to avoid the violation of $u_{const}$. Thus the tracking error is increased because of the more conservative controller.

The effect of active anti-roll bar on chassis roll angle is illustrated in Figure 6(e). Two scenarios are compared in the Figure: a vehicle with active anti-roll bar and a vehicle without roll control system. The peak-values of the roll angle of the uncontrolled vehicle are reduced by the control system, see e.g. at $40s$. The improvement of the roll angle also depends on the controller number. For example, at $30s$ the controller

switches to $n = 1$ to avoid current limit violation. In this case the difference between the roll angles of controlled and uncontrolled vehicle is decreased. Note that at $53s$ the $n = 4$ controller is able to reach an extended enhancement.



(a) Disturbance on the chassis

(b) Tracking performance

(c) Control input $i$

(d) Controller switching sequence
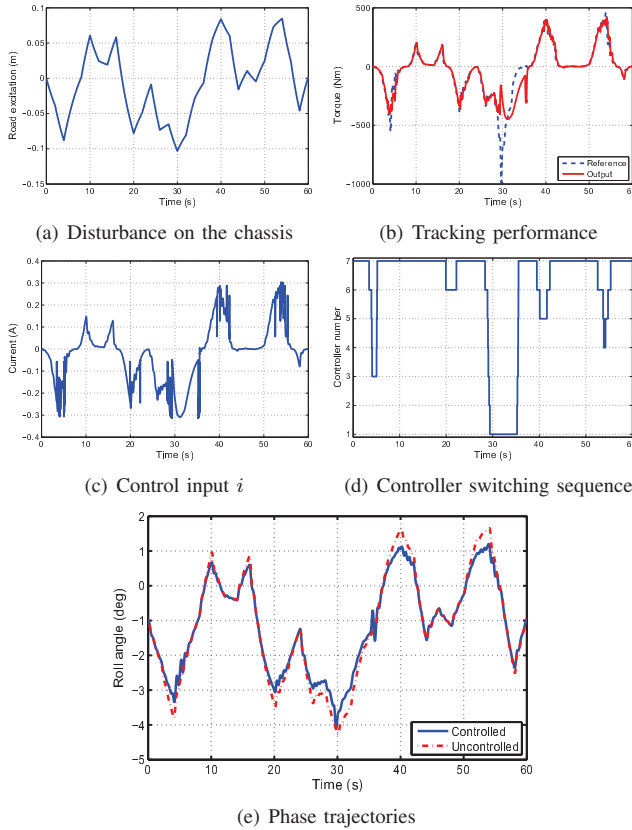
(e) Phase trajectories

Fig. 6. Simulation results of active anti-roll bar system

The presented simulation illustrates the efficiency of the designed actuator control system. The constrained LQ control is able to guarantee the required active torque and to satisfy the current valve constraint simultaneously. The efficient intervention of the controlled actuator improves the roll dynamics of the vehicle.

## VII. Conclusions

The paper proposed an active anti-roll bar actuator control design developed for a light commercial vehicle. The actuator control design fits to the concept of hierarchical control systems. A control-oriented model of the electro-hydraulic actuator is formulated. The conditions of the constrained optimal control problem are formed and a lower-level constrained LQ tracking control is designed. The efficiency of the controlled system is illustrated during simulation examples. The intervention of the designed active anti-roll controller guarantees the enhancement of the roll dynamics and satisfies the input constraint.

## References

[1] G. Wredenhangen and P. Bélanger, "Piecewise-linear LQ control for systems with input constraints," *Automatica*, vol. 30, no. 3, pp. 403–416, 1994.

[2] P. Gáspár, I. Szaszi, and J. Bokor, "The design of a combined control structure to prevent the rollover of heavy vehicles," *European Journal of Control*, vol. 10, no. 2, pp. 148–162, 2004.

[3] Y. Shibahata, "Progress and future direction of chassis control technology," *Annual Reviews in Control*, vol. 29, pp. 151–158, 2005.

[4] D. Cebon, "Interaction between heavy vehicles and roads," *SAE-SP*, vol. 951, 1993.

[5] D. Sampson and D. Cebon, "Active roll control of single unit heavy road vehicles," *Vehicle System Dynamics*, vol. 40, pp. 229–270, 2003.

[6] R. Lin, D. Cebon, and D. Cole, "Optimal roll control of a single-unit lorry," *Proceedings of IMechE, Journal of Automobile Engineering*, vol. 210, pp. 44–55, 1996.

[7] D. Sampson, G. McKevitt, and D. Cebon, "The development of an active roll control system for heavy vehicles," *In Proc. 16th IAVSD Symposium on the Dynamics of Vehicles on Roads and Tracks, Pretoria, South Africa*, pp. 704–715, 1999.

[8] P. Gáspár, I. Szaszi, and J. Bokor, "Rollover stability control in steer-by-wire vehicles based on an LPV method," *International Journal of Heavy Vehicle Systems*, vol. 13, no. 1-2, pp. 125–143, 2006.

[9] D. Odenthal, T. Bunte, and J. Ackermann, "Nonlinear steering and braking control for vehicle rollover avoidance," *Proceedings of European Control Conference, Karlsruhe, Germany*, 1999.

[10] L. Palkovics, A. Semsey, and E. Gerum, "Rollover prevention system for commercial vehicles - additional sensorless function of the electronic brake system," *Vehicle System Dynamics*, vol. 32, pp. 285–297, 1999.

[11] P. Gáspár, I. Szaszi, and J. Bokor, "Reconfigurable control structure to prevent the rollover of heavy vehicles," *Control Engineering Practice*, vol. 13, no. 6, pp. 699–711, 2005.

[12] Y. L. Allan, "Coordinated control of steering and anti-roll bars to alter vehicle rollover tendencies," *Journal of Dynamic Systems, Measurement, and Control*, vol. 124, no. 1, pp. 127–132, 2002.

[13] H. E. Meritt, *Hydraulic control systems*. John Wiley & Sons Inc., 1967.

[14] B. Šulc and J. A. Jan, "Non linear modelling and control of hydraulic actuators," *Acta Polytechnica*, vol. 42, no. 3, pp. 173–182, 2002.

[15] O. Sename, P. Gaspar, and J. Bokor, *Robust Control and Linear Parameter Varying Approaches*. Springer Verlag, Berlin, 2013.

[16] H. Kim and Y. Park, "Investigation of robust roll motion control considering varying speed and actuator dynamics," *Mechatronics*, vol. 14, pp. 35–54, 2004.

[17] K. Zhou, J. Doyle, and K. Glover, *Robust and Optimal Control*. Prentice Hall, 1996.

[18] I. Fialho and G. Balas, "Design of nonlinear controllers for active vehicle suspensions using parameter-varying control synthesis," *Vehicle System Dynamics*, vol. 33, pp. 351–370, 2000.

[19] P. Gáspár, Z. Szabó, and J. Bokor, "Brake control combined with prediction to prevent the rollover of heavy vehicles," *IFAC World Congress, Prague, Czech Republic*, vol. 16, 2005.

[20] S. Zhendong, "Stability of piecewise linear systems revisited," *Annual Reviews in Control*, vol. 34, pp. 221–231, 2010.